

# Characterizing Long-Chain 3-Hydroxy-Acyl-CoA Dehydrogenase Deficiency (LCHADD) Chorioretinopathy Using OCT and OCTA

Xiaohui Hua,<sup>1,2</sup> Tristan T. Hormel,<sup>1</sup> Jie Wang,<sup>1</sup> Dongseok Choi,<sup>1,3</sup> Mark E. Pennesi,<sup>1,4</sup> Melanie B. Gillingham,<sup>5</sup> and Yali Jia<sup>1,2</sup>

<sup>1</sup>Casey Eye Institute, Oregon Health & Science University, Portland, Oregon, United States

<sup>2</sup>Department of Biomedical Engineering, Oregon Health & Science University, Portland, Oregon, United States

<sup>3</sup>OHSU-PSU School of Public Health, Biostatistics, Oregon Health & Science University, Portland, Oregon, United States

<sup>4</sup>Retina Foundation of the Southwest, Dallas, Texas, United States

<sup>5</sup>Department of Molecular and Medical Genetics, Oregon Health & Science University, Portland, Oregon, United States

Correspondence: Yali Jia, Casey Eye Institute, Oregon Health & Science University, 515 SW Campus Dr., Portland, OR 97239, USA;  
jaya@ohsu.edu.

Received: March 11, 2025

Accepted: August 27, 2025

Published: September 24, 2025

Citation: Hua X, Hormel TT, Wang J, et al. Characterizing long-chain 3-hydroxy-acyl-CoA dehydrogenase deficiency (LCHADD) chorioretinopathy using OCT and OCTA. *Invest Ophthalmol Vis Sci*. 2025;66(12):57.

<https://doi.org/10.1167/iovs.66.12.57>

**PURPOSE.** To characterize structural and microvascular alterations in chorioretinopathy in patients with long-chain 3-hydroxyacyl-CoA dehydrogenase deficiency (LCHADD) using optical coherence tomography (OCT) and OCT angiography (OCTA).

**METHODS.** Thirty-six eyes from 19 patients with LCHADD were evaluated and categorized into six stages of increasing severity. Avanti and Solix OCTA devices were used to scan acquire 3 × 3-mm macular scans of the eyes. The thicknesses of the inner retina, outer retina, and choroid were measured from OCT scans. Vessel density (VD) and nonperfusion area (NPA) were calculated from en face projection-resolved OCTA in four slabs: the superficial vascular complex, intermediate capillary plexus, deep capillary plexus (DCP), and choriocapillaris (CC). The correlations (Spearman's rank) between these structural and angiographic metrics and traditional clinical metrics (the LCHADD severity, best-corrected visual acuity [BCVA], and plasma acylcarnitines) were investigated.

**RESULTS.** Pronounced thinning in the outer retina and choroid was observed, along with marked VD loss and increased NPA in the DCP and CC at severe stages. The outer retinal and choroidal thicknesses correlated with all traditional clinical metrics, VD/NPA in the DCP and CC were significantly correlated with the LCHADD severity and BCVA, and only VD/NPA in the CC were associated with plasma acylcarnitines.

**CONCLUSIONS.** Combined OCT/OCTA imaging enables visualization and quantification of structural and microvascular alterations in the chorioretinal slabs at different stages of LCHADD. The pathology of LCHADD impacts the deeper retinal plexuses more than the inner layers. OCT and OCTA parameters may improve understanding of the pathological changes in LCHADD chorioretinopathy and aid in monitoring disease progression.

Keywords: LCHADD chorioretinopathy, OCT, OCTA

Long-chain 3-hydroxyacyl-CoA dehydrogenase deficiency (LCHADD) is a rare genetic disorder that impairs mitochondrial fatty acid  $\beta$ -oxidation, leading to significant alteration in retinal metabolism.<sup>1</sup> Metabolic disorders like LCHADD have profound effects on both the structure and vasculature of the retina, often presenting as chorioretinopathy, which can result in vision impairment or loss.<sup>2–5</sup> Visualizing and quantifying tissue changes and vascular abnormalities could help elucidate LCHADD chorioretinopathy etiology and development, as well as improve the assessment of experimental treatments.

Several imaging modalities have been previously applied to observe such changes among patients with LCHADD. Fundus autofluorescence (FAF), optical coherence tomography (OCT), and fluorescein angiography (FA) are common imaging techniques in the initial diagnosis and monitoring of LCHADD chorioretinopathy progression. While FAF

can illustrate changes in retinal pigment epithelium (RPE), it is limited to capturing the lipofuscin distribution in the RPE, leaving other retinal structures not discernible.<sup>6,7</sup> OCT provides reliable, depth-resolved structural information about the retina and has been instrumental in revealing abnormal layers affected in LCHADD, but it is limited by its inability to visualize vasculature.<sup>8–10</sup> FA has been previously used for the qualitative evaluation of vascular changes in LCHADD, but it is an invasive technique that is not depth-resolved, making it unable to differentiate between retinal layers.<sup>10,11</sup>

Alternatively, OCT angiography (OCTA) is a fast, noninvasive imaging technique that provides volumetric data, enabling precise localization and delineation of pathology while capturing both structural and angiographic information.<sup>12–14</sup> Each OCTA scan produces coregistered OCT and OCTA volumes. The OCT volume can be used to evaluate



structural changes in tissue, while the OCTA volume can be used to assess vascular changes. Combined OCT/OCTA imaging has demonstrated utility in identifying structural and microvascular changes in various retinopathies.<sup>15,16</sup>

Previously, we detected choroidal neovascularization at an early stage of LCHADD;<sup>17</sup> however, the microvascular circulation in the inner retinal plexuses and choriocapillaris (CC) remains unclear. Thus, in this study, we present the first comprehensive assessment of structural and microvascular anatomy in LCHADD chorioretinopathy using OCT/OCTA. We characterized variations in the structural changes in the inner retina, outer retina, and choroid, as well as the microvasculature across all retinal plexuses and the CC across the entire LCHADD severity scale. Additionally, we investigated the correlations of these parameters with LCHADD severity, best-corrected visual acuity (BCVA), and plasma acylcarnitines (a traditional LCHADD biomarker of partially oxidized long-chain fatty acids). This study may provide a better understanding of the pathological changes in LCHADD and determine biomarkers for disease progression.

## METHODS

### Study Population

Participants were recruited for the Natural History of LCHADD Retinopathy study, a two-site prospective cohort study conducted at Oregon Health & Science University (OHSU) and the University of Pittsburgh Medical Center (UPMC). The study was approved by the institutional review board of UPMC (IRB# PRO19040142). OHSU deferred oversight to UPMC. The participants included in this report were all evaluated at the Casey Eye Institute, OHSU. Informed consent was obtained from all participants or their guardians, and the study adhered to the Declaration of Helsinki.<sup>18</sup>

The diagnosis of LCHADD was confirmed by a review of medical records and the identification of two pathogenic mutations in the *HADHA* gene. All participants underwent a comprehensive ophthalmic examination, which included BCVA assessment using Snellen charts, with results converted to logMAR units. Spherical equivalence was calculated as the spherical diopter (D) plus one-half of the cylindrical dioptic power. Axial length was measured using the IOL Master 500 (Carl Zeiss Meditec, Dublin, CA, USA). All participants were staged according to the updated staging system proposed by our team, Wongchaisuwat et al.<sup>19</sup> All patients were categorized into six stages. In stage 1, both the retina and choroid appear normal; stage 2A is characterized by a normal to thickened RPE-Bruch complex in the macula, with mild attenuation (i.e., thinning, but not complete loss) of the ellipsoid zone (EZ)/RPE and a normal choroid, while stage 2B shows similar changes, but changes can extend beyond the vascular arcades into the periphery. In stage 3A, there is progressive outer retinal attenuation with a normal or mildly thinned choroid. Stage 3B involves more extensive progressive atrophy of both the outer retina and choroid but sparing the central fovea. Finally, stage 4 is marked by extensive outer retinal and choroidal atrophy, with the central fovea largely spared.

Participants' images were excluded when the following appeared: (1) other ocular or systemic conditions affecting the retina rather than LCHADD; (2) previous intraocular surgery, except for uncomplicated cataract extraction with posterior chamber intraocular lens implantation; and (3) inability to maintain fixation

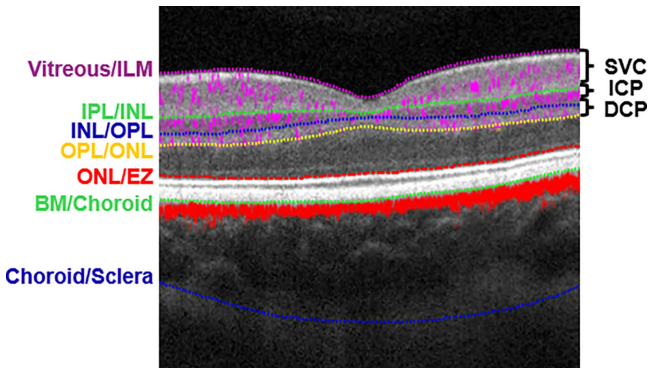


**FIGURE 1.** Cross-sectional OCT and projection-resolved OCT angiography (PR-OCTA) images from the left eye of a healthy participant show the relationship between the chorioretinal vascular plexuses and anatomic layers. The color-coded flow signal (purple: retina; red: choroid) overlays the gray-scaled reflectance signal.

for scanning that led to OCT/OCTA data acquisition unsuccessfully.

### Data Acquisition and Processing

All participants were scanned in a  $3 \times 3$ -mm area centered on the fovea using two commercial OCTA systems: (1) Avanti (Visionix USA, Lombard, IL, USA) with an 840-nm central wavelength and a 70-kHz axial scan rate and (2) Solix (Visionix USA, Lombard, IL, USA) with a center wavelength of 840 nm and a 120-kHz axial scan rate. On the Avanti system, a  $3 \times 3$ -mm OCT/OCTA volume consists of 304 B-frames, and each B-frame contains 304 A-lines. With a faster scanning rate, the Solix system can achieve a higher scanning density with a  $3 \times 3$ -mm OCT/OCTA volume consisting of 400 B-frames, and each B-frame contains 400 A-lines. In both Avanti and Solix systems, flow signals were detected using the commercial version of the split-spectrum amplitude-decorrelation angiography algorithm,<sup>12</sup> and then the projection-resolved OCTA algorithm was used to suppress the projection artifacts from the superficial plexuses.<sup>20</sup>

OCT/OCTA volumes were processed using the Center for Ophthalmic Optics & Lasers-Angiography Reading Toolkit (COOL-ART) software.<sup>21</sup> The layer boundaries of the vitreous/inner limiting membrane (ILM), the inner plexiform layer (IPL)/inner nuclear layer (INL), INL/outer plexiform layer (OPL), OPL/outer nuclear layer (ONL), ONL/EZ, Bruch's membrane (BM)/choroid, and choroid/sclera were segmented automatically (Fig. 1). Any segmentation errors that occurred were corrected manually.

The inner retinal slab was defined as the region between the ILM and the inner boundary of the INL. The outer retinal slab was defined between the inner boundary of the OPL and BM to eliminate interference from the Henle fiber layer.<sup>22</sup> The choroid was located between the BM and the inner boundary of the sclera. Three vascular plexuses were the superficial vascular complex (SVC), the intermediate capillary plexus (ICP), and the deep capillary plexus (DCP). The SVC was located within the inner 80% of the ganglion cell complex (GCC: from the inner ILM to the outer boundary of IPL). The ICP spanned from the outer 20% of the GCC to the inner 50% of the INL. The DCP was identified from the outer 50% of the INL to the OPL. The CC slab was segmented from a 10- $\mu\text{m}$ -thick slab below the BM. These segmentation

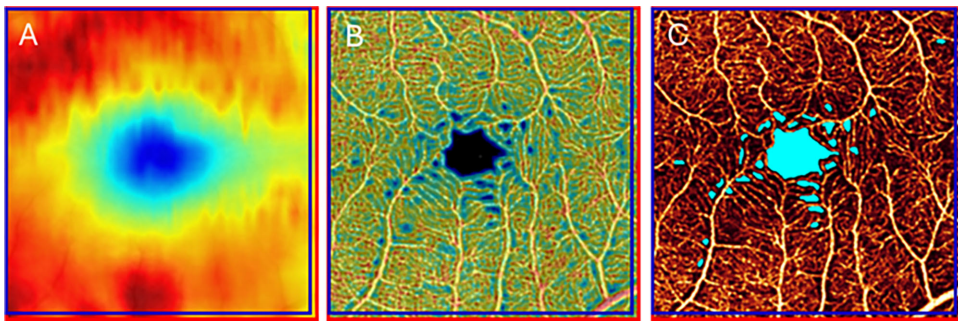


**FIGURE 2.** Illustration of magnification uncorrected and corrected measurement area for thickness (A), VD (B), and NPA (C) of the SVC. The red square represents the magnification uncorrected measurement area, while the blue square represents the magnification corrected measurement area corresponding to the true 3 × 3-mm region.

results were used for thickness, vessel density (VD), and nonperfusion area (NPA) generation.

Thickness measurements can assess structural changes in the retina and choroid due to LCHADD. Thickness maps of the inner retina, outer retina, and choroid were generated by measuring the distances between the boundaries of these layers. The thickness values used for statistical analysis were obtained by averaging the thicknesses across the entire map.

VD and NPA are two representative OCTA parameters used to evaluate microvascular changes. En face OCTA of the SVC, ICP, DCP, and CC was generated from the corresponding OCTA slabs using the maximum projection approach.<sup>23</sup> In each en face OCTA, retinal vasculature was enhanced using the local contrast, and then Otsu's method was applied to generate the binary vascular mask.<sup>24,25</sup> The VD of each microvascular slab was measured as a percentage of the area occupied by the OCTA signal.

NPA measures regions where blood flow is absent, often due to vascular damage. A previously developed deep learning method,<sup>26</sup> capable of compensating for artifacts, was used to measure NPA on en face OCTA angiograms of the SVC, ICP, and DCP. The NPA of CC was detected by applying a threshold to the CC VD image based on its local contrast. The foveal avascular zone (FAZ) was included in the detected NPA.

Thickness, VD, and NPA were measured within the actual 3 × 3-mm square area centered on the FAZ (Fig. 2). The image scale of this area was adjusted based on the average axial length of healthy eyes of normal controls ( $L_a = 23.8$  mm) (Equation 1).<sup>27</sup> The actual resolution of each pixel in width and height is calculated by

$$r_{pix} = (3.0 \times L) / (L_a \times S_p) \quad (1)$$

where  $L$  is the axial length of each eye, and  $S_p$  is the image size (in pixels) for both width and height (equal in this study). Since the magnification version does not affect the depth resolution, and the VD measures the percentage of the pixels occupied by the vessels, the thickness and VD values do not need to be adjusted by the actual pixel resolution but need to be measured within the adjusted actual 3 × 3-mm area. The NPA was adjusted based on the actual pixel resolution (in pixel/mm<sup>2</sup>) (Equation 2) by

$$NPA = N \times r_{pix}^2 \quad (2)$$

where  $N$  is the total number of pixels of NPA within the adjusted actual 3 × 3-mm area.

Elevated plasma long-chain 3-hydroxy acylcarnitines serve as a screening and diagnostic biomarker for LCHADD, and we have reported a relationship between increased acylcarnitines and lower visual acuity.<sup>28</sup> The specific acylcarnitine species associated with LCHADD on a comprehensive acylcarnitine profile include C14:0-OH, C14:1-OH, C16:0-OH, C16:1-OH, C18:0-OH, C18:1-OH, and C18:2-OH.<sup>29,30</sup> Plasma from a fasting blood sample was analyzed for acylcarnitines by liquid chromatography-tandem mass spectrometry, and the LCHADD-specific species were quantified for all participants. Principal components analysis (PCA) was used to summarize these acylcarnitine species and reduce data dimensionality,<sup>31</sup> representing overall plasma long-chain 3-OH acylcarnitine concentrations for each participant. The principal component 1 (PCA1) explained 88% of the variation in acylcarnitines and is used as a biomarker of disease severity, with higher PCA1 indicating higher long-chain 3-hydroxy acylcarnitines and lower LCHAD enzymatic activity.

## Statistical Methods

The statistical analyses were performed with SPSS 23.0 (IBM Corporation, Chicago, IL, USA). Spearman rank-order correlation analysis was used to test the correlation between OCT and OCTA parameters with LCHADD severity, BCVA, and plasma acylcarnitines. Bonferroni correction was applied separately to the OCT and OCTA analyses to adjust for multiple testing. The adjusted significance thresholds were set at  $P < 0.0056$  (0.05/9 tests) for the OCT parameters and  $P < 0.0021$  (0.05/24 tests) for the OCTA parameters, based on the number of tests in each group. To account for the intrasubject correlation between eyes, linear mixed models (LMMs) with random intercepts for participants were used.

## RESULTS

### Study Population

Nineteen participants diagnosed with LCHADD out of the 40 were included in this analysis, and 36 eyes were evaluated in this study. Participants ranged in age from 2 to 30 years at the time of evaluation. Due to poor scan quality, two left eyes were excluded from the analysis. Based on the LCHADD score system that incorporated a comprehensive assessment, including fundus changes, OCT

**TABLE 1.** Participants' Characteristics and the Measurements of OCT and OCTA

| Parameter                                  | LCHADD         |              |                |                |               |                |
|--|----------------|--------------|----------------|----------------|---------------|----------------|
|  | Stage 1        | Stage 2A     | Stage 2B       | Stage 3A       | Stage 3B      | Stage 4        |
| Participants, <i>n</i>                     | 6              | 4            | 4              | 1              | 1             | 3              |
| Eyes, <i>n</i>                             | 12             | 8            | 7              | 2              | 2             | 5              |
| Age, y                                     | 12.1 ± 3.5     | 10.1 ± 6.3   | 15.1 ± 3.3     | 18.8           | 24.8          | 25.5 ± 8.1     |
| SE (D)                                     | -0.7 ± 1.56    | -1.7 ± 3.54  | -1.8 ± 2.18    | -3.88 ± 6.19   | -0.31 ± 0.09  | -2.2 ± 2.46    |
| AL (mm)                                    | 23.22 ± 0.26   | 22.51 ± 0.7  | 24.39 ± 0.51   | 23.41 ± 0.13   | 22.76 ± 0.03  | 25.22 ± 0.57   |
| BCVA (logMAR)                              | -0.11 ± 0.07   | -0.05 ± 0.08 | 0.23 ± 0.35    | 0.2            | 0.35 ± 0.5    | 0.9 ± 0.65     |
| Plasma acylcarnitines PCA1                 | -1.89 ± 2.04   | -0.65 ± 1.27 | 2.21 ± 0.51    | 2.37           | 1.19          | 2.42 ± 0.88    |
| Structural OCT thickness measurements (μm) |                |              |                |                |               |                |
| Inner retina                               | 148.88 ± 7.54  | 141.27 ± 8.7 | 134.11 ± 24.63 | 167.07 ± 0.33  | 177.06 ± 6.98 | 141.96 ± 14.84 |
| Outer retina                               | 181.03 ± 7.12  | 186.14 ± 5.5 | 156.68 ± 14.5  | 123.48 ± 3.55  | 103.2 ± 26.1  | 56.64 ± 20.47  |
| Choroidal                                  | 257.92 ± 42.26 | 256 ± 40.35  | 237.03 ± 74.27 | 131.53 ± 14.96 | 71.83 ± 15.1  | 55.2 ± 21.32   |
| OCTA measurements                          |                |              |                |                |               |                |
| SVC VD                                     | 0.47 ± 0.01    | 0.46 ± 0.02  | 0.47 ± 0.01    | 0.48 ± 0.01    | 0.46 ± 0.01   | 0.4 ± 0.07     |
| ICP VD                                     | 0.5 ± 0.02     | 0.48 ± 0.01  | 0.5 ± 0.02     | 0.5 ± 0.01     | 0.49 ± 0.01   | 0.41 ± 0.1     |
| DCP VD                                     | 0.49 ± 0.02    | 0.49 ± 0.02  | 0.5 ± 0.03     | 0.48           | 0.45 ± 0.03   | 0.31 ± 0.1     |
| CC VD                                      | 0.54 ± 0.01    | 0.53 ± 0.01  | 0.53 ± 0.01    | 0.36 ± 0.01    | 0.28 ± 0.18   | 0.21 ± 0.04    |
| SVC NPA, mm <sup>2</sup>                   | 0.1 ± 0.07     | 0.18 ± 0.06  | 0.09 ± 0.06    | 0.08 ± 0.07    | 0.24 ± 0.01   | 1.14 ± 1.31    |
| ICP NPA, mm <sup>2</sup>                   | 0.02 ± 0.01    | 0.09 ± 0.05  | 0.02 ± 0.03    | 0.03 ± 0.03    | 0.03 ± 0.04   | 1.21 ± 1.66    |
| DCP NPA, mm <sup>2</sup>                   | 0.02 ± 0.02    | 0.11 ± 0.09  | 0.05 ± 0.07    | 0.16 ± 0.03    | 0.4 ± 0.53    | 2.94 ± 1.78    |
| CC NPA, mm <sup>2</sup>                    | 0              | 0            | 0.02 ± 0.05    | 1.69 ± 0.11    | 3.16 ± 2.63   | 5.08 ± 0.71    |

AL, axial length; BCVA, best-corrected visual acuity; CC, choriocapillaris; D, diopters; DCP, deep capillary plexus; ICP, intermediate capillary plexus; NPA, nonperfusion area; SE, spherical equivalent; SVC, superficial vascular complex; VD, vessel density.

characteristics, FAF, and full-field electroretinography findings,<sup>19</sup> all LCHADD eyes were scored by an ophthalmologist into one of the six stages of LCHADD chorioretinopathy (Table 1).

## Structural OCT Findings and Analyses

The cross-sectional images revealed thinning of the outer retina and choroid as LCHADD severity increased, and corre-

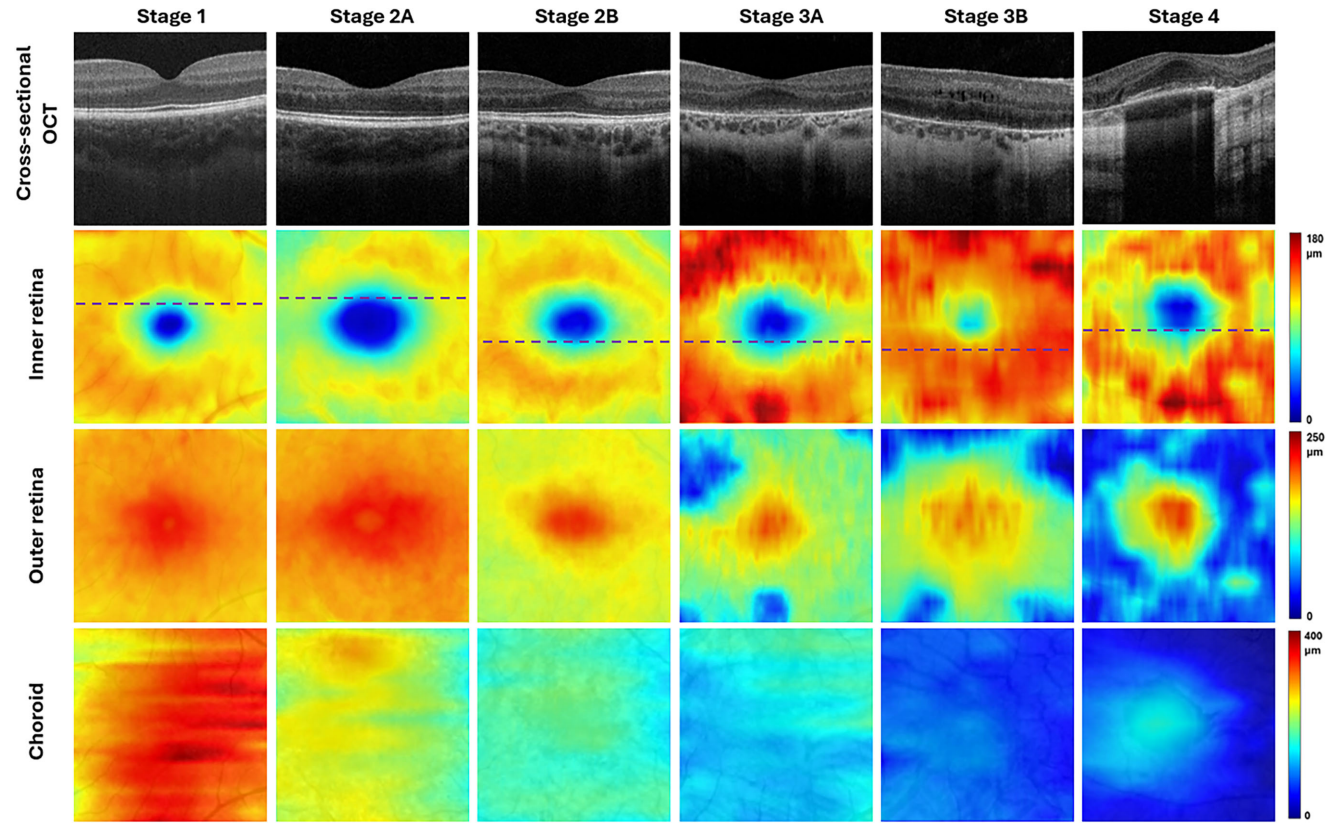


**FIGURE 3.** The 3 × 3-mm macular structural OCT images at different stages of LCHADD severity. Cross-sectional OCT images (row 1) correspond to the location indicated by the *dark purple dashed line* in the inner retina (row 2). The thicknesses of the outer retina (row 3) and choroid (row 4) decrease significantly in the advanced stages, whereas the inner retina shows a slight increase in thickness in the severe stages.

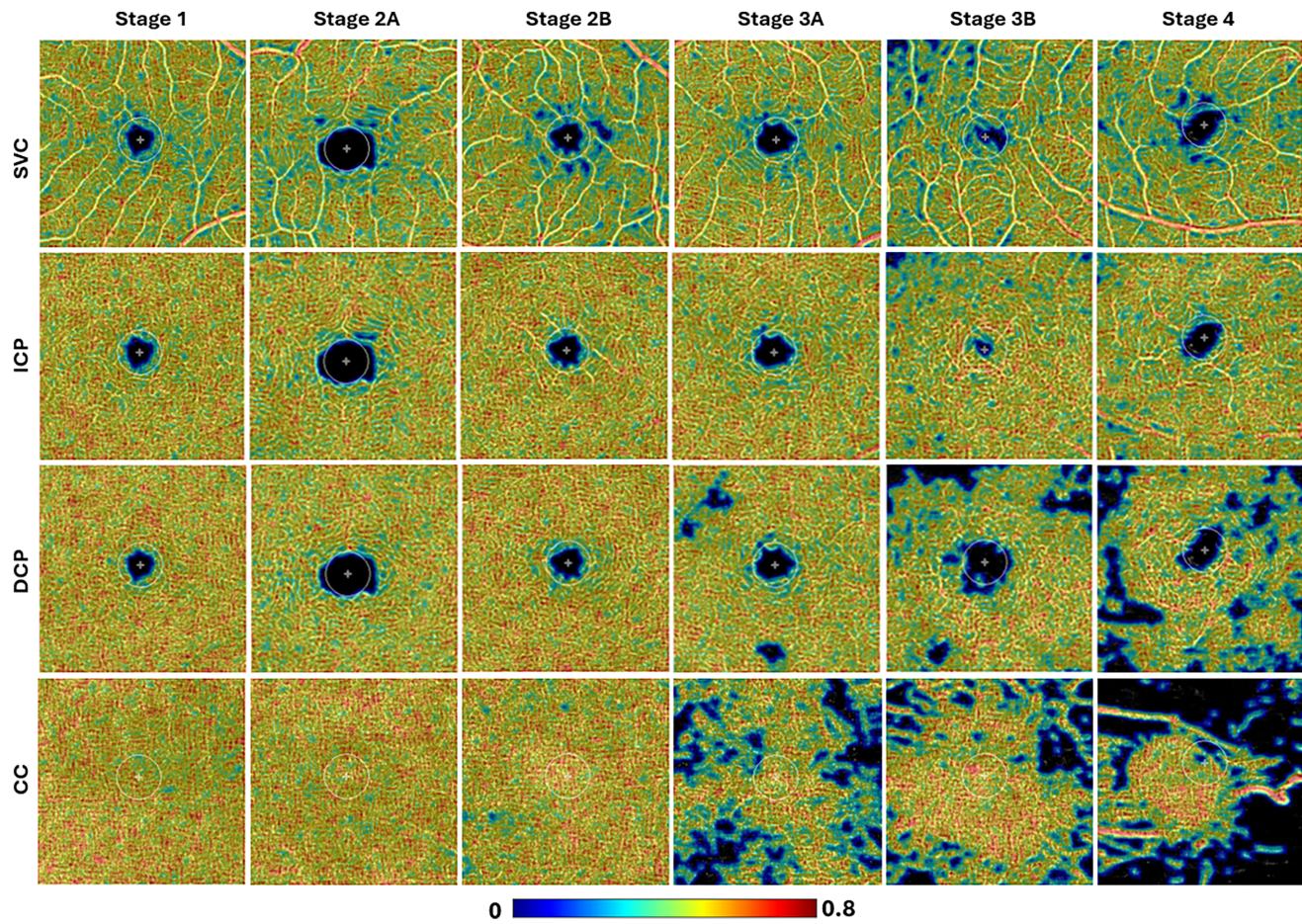


**FIGURE 4.** VD maps of eyes with LCHADD at different severity stages show significant VD loss in the DCP (row 3) and CC (row 4), especially in the last three stages. In contrast, the SVC (row 1) and ICP (row 2) show relatively stable VD across all stages compared to the DCP and CC.

sponding structural alterations were observed in thickness maps across different slabs (Fig. 3, Supplementary Fig. S1). In particular, the thinning of the outer retina became significantly more pronounced from stage 2B to stage 4 compared to stage 1 and stage 2A. Choroidal thinning was evident, with a progressive reduction at each advancing level of LCHADD severity, starting from stage 1 (Table 1). In contrast, the thickness of the inner retina showed a mild increase in the advanced stages (3A, 3B, and 4) compared to the early stages (1, 2A, and 2B). To quantify these changes, the thickness difference ( $\Delta$ ) was measured, representing the mean percentage changes in thickness between the two stages. We compared the earliest (stage 1) and the most advanced stage (stage 4). The thickness of the inner retina remained relatively stable ( $\Delta = -4.6\%$ ) compared to the more substantial reductions observed in the outer retina ( $\Delta = -68.7\%$ ) and choroid ( $\Delta = -78.6\%$ ).

### OCTA Findings and Analyses

VD maps across the three retinal vascular/capillary plexuses (SVC, ICP, and DCP) and the CC revealed varying levels of VD corresponding to different stages of LCHADD severity (Fig. 4). A significant reduction in VD was observed in the DCP, beginning at stage 3A and becoming more pronounced in the more severe stages compared to stage 1, stage 2A, and

stage 2B (Table 1). In contrast, the superficial slabs (SVC and ICP) exhibited less notable reductions in VD (Fig. 4, rows 1 and 2). The CC density started to decline from stage 3A and decreased with increasing LCHADD severity. These findings underscore the differential impact of LCHADD on various vascular plexuses, with the most substantial VD reductions occurring in the DCP and CC and a more pronounced loss in the CC compared to the SVC, ICP, and DCP at advanced stages.

The NPA maps illustrated the extent of perfusion area loss in LCHADD (Fig. 5). In the SVC and ICP, the NPA remained relatively stable across different stages of LCHADD severity. However, in the DCP, there were no significant changes in the NPA during the early stages (1, 2A, and 2B). The NPA then increased noticeably in the advanced stages (3A, 3B, and 4) compared to earlier stages. Similarly, in the CC, NPA rose dramatically in the advanced stages, while in the earlier stages, NPA values were nearly zero (Table 1). Overall, we observed a clear increase in NPA with LCHADD severity in both the DCP and CC, with the most significant rise occurring in the CC (Fig. 5, rows 3 and 4).

In general, the analyses of VD and NPA revealed distinct vascular patterns across LCHADD stages. The vasculature in the SVC and ICP remained relatively stable from stage 1 to stage 4, and the three retinal vascular/capillary plexuses, along with the CC, appeared normal during the first three

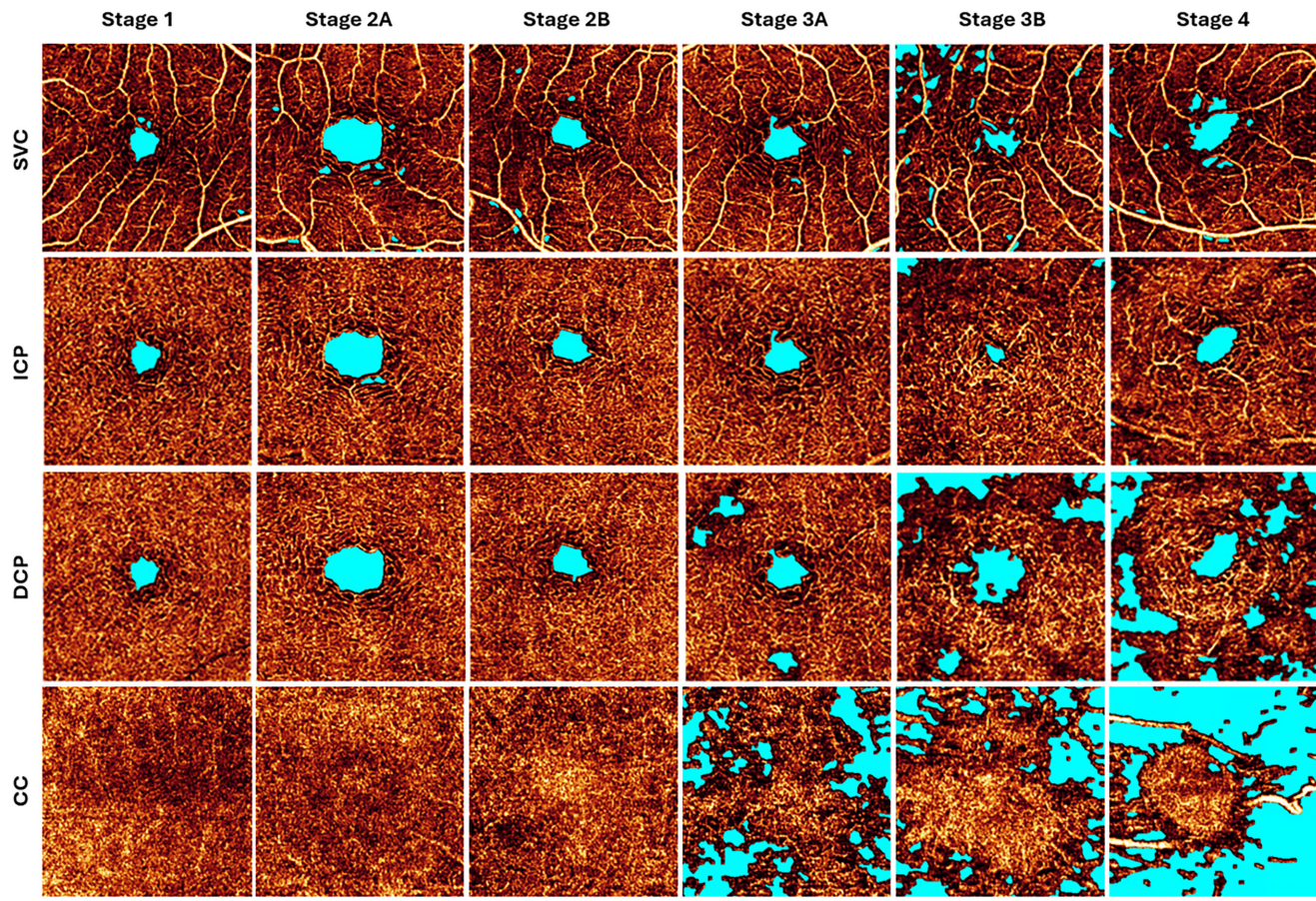


**FIGURE 5.** NPA maps of eyes with LCHADD at different severity stages show a noticeable increase in NPA in the DCP (row 3) and CC (row 4) slabs after stage 3A, with the most significant rise occurring in the CC. In contrast, the SVC (row 1) and ICP (row 2) show lower NPA than the DCP and CC in severe stages.

**TABLE 2.** Spearman Correlation Coefficients of OCT Parameters With LCHADD Severity, Best-Corrected Visual Acuity, and Plasma Acylcarnitines

| Characteristic      | Inner Retina Thickness | Outer Retina Thickness | Choroidal Thickness |
|---------------------|------------------------|------------------------|---------------------|
| LCHADD severity     | 0.03                   | -0.77**                | -0.66**             |
| BCVA                | -0.03                  | -0.72**                | -0.65**             |
| Acylcarnitines PCA1 | -0.08                  | -0.54**                | -0.41*              |

\*  $P < 0.005$ .

\*\*  $P < 0.001$ .

stages. However, vascular abnormalities in the DCP and CC layers emerged and progressively worsened with increasing disease severity (3A to 4), with deeper layers exhibiting more pronounced vascular loss.

### Correlation Analysis

The Spearman correlation coefficients of inner retinal thickness, outer retinal thickness, and choroidal thickness with LCHADD severity, BCVA, and plasma acylcarnitines PCA1 were analyzed (Table 2; Supplementary Fig. S2). Outer retinal and choroidal thicknesses exhibited significant correlations with LCHADD severity, BCVA, and plasma acylcarnitines PCA1 ( $P < 0.005$ ), with outer retinal thickness showing stronger correlations. In contrast, inner retinal thickness did not display any statistically significant correlation with

LCHADD severity, BCVA, and plasma acylcarnitines PCA1, indicating that the inner retina remains relatively unaffected in thickness as LCHADD severity increases.

Significant correlations were observed between VD/NPA in the DCP and CC with both LCHADD severity and BCVA (Table 3). However, VD/NPA in SVC correlated only with LCHADD severity, while those in the ICP were only correlated with BCVA. Notably, only VD/NPA in the CC significantly correlated with the plasma acylcarnitines PCA1 ( $\rho = -0.56, P < 0.001$  and  $\rho = 0.4, P < 0.002$ , respectively). Among all the OCTA parameters, the VD/NPA in the CC showed the strongest correlations with LCHADD severity, BCVA, and plasma acylcarnitines PCA1. Furthermore, the correlation coefficients between VD/NPA and both LCHADD severity and BCVA increased with retinal depth, reaching their peak in the CC, indicating that deeper retinal layers are

**TABLE 3.** Spearman Correlation Coefficients of OCTA Parameters With LCHADD Severity, Best-Corrected Visual Acuity, and Plasma Acylcarnitines

| Characteristic      | SVC VD | ICP VD | DCP VD  | CC VD   | SVC NPA | ICP NPA | DCP NPA | CC NPA |
|---------------------|--------|--------|---------|---------|---------|---------|---------|--------|
| LCHADD severity     | -0.35* | -0.24  | -0.46*  | -0.81** | 0.4*    | 0.33    | 0.56**  | 0.73** |
| BCVA                | -0.15  | -0.3*  | -0.51** | -0.68** | 0.26    | 0.37*   | 0.57**  | 0.64** |
| Acylcarnitines PCA1 | -0.29  | -0.02  | -0.15   | -0.56** | 0.23    | 0.08    | 0.21    | 0.4*   |

\*  $P < 0.002$ .

\*\*  $P < 0.001$ .

more susceptible to the effects of LCHADD pathology. The associations identified in the Spearman's correlation analyses in OCT and OCTA parameters remained significant after adjusting for intrasubject correlation using LMMs.

## DISCUSSION

In this study, we characterized structural and microvascular changes in patients with LCHADD using OCT and OCTA. Quantitative changes were observed in both the chorioretinal structure and microvasculature. To the best of our knowledge, this is the first comprehensive study to evaluate pathologic changes across multiple structural slabs (inner retina, outer retina, and choroid) and vascular plexuses/complexes (SVC, ICP, DCP, and CC) in LCHADD chorioretinopathy. Our findings demonstrate the following: (1) tissue thinning in advanced stages of LCHADD in the outer retina and choroid; (2) marked capillary dropout in the DCP and CC in later stages without a corresponding reduction in the SVC and ICP; (3) a strong correlation between outer retinal and choroidal thicknesses and LCHADD severity, BCVA, and plasma acylcarnitines; and (4) a strong correlation between VD/NPA in the CC and LCHADD severity, BCVA, and plasma acylcarnitines.

Previous studies have reported retinal and choroidal structural changes in LCHADD. Boese et al.<sup>7</sup> demonstrated progressive outer retinal atrophy, while Tyni et al.<sup>32</sup> and Dulz et al.<sup>33</sup> identified RPE involvement in LCHADD retinopathy. In LCHADD, insufficient nutrient delivery due to impaired metabolism likely contributes to photoreceptor and RPE degeneration.<sup>34</sup> Increased RPE degeneration has been observed in LCHADD mouse models.<sup>35</sup> Alternatively, higher plasma 3-hydroxy-acylcarnitines have correlated with lower visual acuity and advanced stages of retinopathy, suggesting a potentially toxic effect on the RPE/CC.<sup>36,37</sup> Additionally, previous studies have reported CC atrophy in LCHADD.<sup>1,7,32</sup> However, although these studies have provided valuable insights into LCHADD, the pathology underlying the development of chorioretinopathy in this condition remains incompletely understood and needs further investigation.

In this study, beyond assessing structural changes in the retinal tissue, we also incorporated the choroidal slab and provided quantitative analysis for both retinal and choroidal layers. Consistent with previous reports of outer retinal structural loss, we confirmed significant thinning of the outer retina, particularly beyond stage 2B, with the reduction becoming more pronounced as LCHADD severity progressed. This might be due to damage to the photoreceptor layer and the RPE. In addition, we observed progressive choroidal thinning with the advancement of LCHADD, highlighting its involvement in the disease process. These changes were observed in cross-sectional OCT scans (Fig. 3, row 1). This finding is consistent with the new score system

relating to OCT structural changes,<sup>19</sup> which we further confirmed using thickness maps (Fig. 3, rows 3 and 4).

We observed a noticeable VD reduction and a corresponding NPA increase in both the DCP and CC with increasing LCHADD severity, with more extensive capillary dropout in the CC than the DCP (Fig. 4, rows 3 and 4; Fig. 5, rows 3 and 4). These vascular changes were prominent in advanced stages, while the vasculature remained relatively intact in earlier stages (1–2). This progression followed a similar pattern to outer retinal and choroidal thinning, which was also limited in the first three stages of disease development. Together, these observations suggest a pattern of disease progression in which atrophic changes may either originate in or more strongly affect deeper tissue, beginning in more advanced disease stages. This preferential susceptibility of the outer retina and choroid may result from impaired mitochondrial metabolism, given the critical role of mitochondrial fatty acid  $\beta$ -oxidation in RPE function.<sup>19,32,38</sup> Additionally, elevated plasma 3-hydroxy acylcarnitines may exert a toxic effect on the RPE and CC.<sup>36,37</sup> Impaired mitochondrial function can lead to RPE and choroidal dysfunction, compromising support for photoreceptors and the choroidal vasculature, ultimately resulting in outer retinal and choroidal atrophy.

Our correlation analysis assessed the relationship between OCT and OCTA parameters with LCHADD severity, BCVA, and plasma acylcarnitines to identify the efficacy of our approaches (OCT/OCTA) for monitoring and diagnosing LCHADD chorioretinopathy. Outer retinal and choroidal thicknesses showed strong, consistent correlations with LCHADD severity, BCVA, and plasma acylcarnitines, while the inner retina showed no significant correlations. Additionally, VD/NPA in DCP and CC were significantly correlated with BCVA and LCHADD severity, but only VD/NPA in the CC were associated with the plasma acylcarnitines. Overall, outer retinal thickness, choroidal thickness, and VD/NPA in the CC are more sensitive biomarkers of various LCHADD chorioretinopathy phenotypes than anterior structural thickness and inner retinal vascular metrics.

Although this study provided insight into the progression of LCHADD chorioretinopathy, including structural alterations and microvascular changes in the chorioretinal slabs, some limitations still need to be addressed in future studies. First, the small data size of each stage of LCHADD makes it hard to compare the difference in OCT and OCTA parameters among LCHADD at different stages. Second, the age range of participants included in this analysis was quite broad, so the impact of age on LCHADD progression should be considered. Third, its cross-sectional design limits our ability to assess longitudinal changes in OCT and OCTA parameters over time, restricting the evaluation of these biomarkers' utility for long-term monitoring of LCHADD.

In conclusion, we demonstrate that tissue structure loss and vascular perfusion decline emerge and progressively

deteriorate in the advanced stages, with deeper layers, particularly the outer retina and choroid, more susceptible to damage. Our findings suggest that OCT and OCTA parameters can monitor disease progression and aid in diagnosing LCHADD chorioretinal stage, providing deeper insights into the pathology of LCHADD chorioretinopathy.

### Acknowledgments

Supported by grants from the National Institutes of Health (R01 HD 095968, R01 EY 036429, R01 EY035410, R01 EY024544, R01 EY027833, R01 EY031394, R43EY036781, P30 EY010572, T32 EY023211, UL1TR002369); the Jennie P. Weeks Endowed Fund; the Malcolm M. Marquis, MD Endowed Fund for Innovation; Unrestricted Departmental Funding Grant and H. James and Carole Free Catalyst Award from Research to Prevent Blindness (New York, NY); Edward N. & Della L. Thome Memorial Foundation Award; and the Bright Focus Foundation (G2020168, M20230081).

**Disclosure:** **X. Hua**, None; **T.T. Hormel**, Ifocus Imaging (I); **J. Wang**, Visionix/Optovue (P, R), Roche/Genentech (P, R), Ifocus Imaging (I); **D. Choi**, None; **M.E. Pennesi**, None; **M.B. Gillingham**, Reneo Pharmaceutical (R), Nestle Health Science (R), Ultragenyx Pharmaceutical (C), Travere Pharmaceutical (C), Nutricia (C), Vitaflow (C); **Y. Jia**, Visionix/Optovue (P, R), Roche/Genentech (P, R, F), Ifocus Imaging (I, P), Optos (P), Boeringer Ingelheim (C), Kugler (R)

### References

- Rigaudiere F, Delouvrier E, Le Gargasson JF, Milani P, Ogier de Baulny H, Schiff M. Long-chain 3-hydroxyacyl-CoA dehydrogenase (LCHAD) deficiency and progressive retinopathy: one case report followed by ERGs, VEPs, EOG over a 17-year period. *Doc Ophthalmol*. 2021;142(3):371–380.
- Country MW. Retinal metabolism: a comparative look at energetics in the retina. *Brain Res*. 2017;1672:50–57.
- Pournaras CJ, Rungger-Brandle E, Riva CE, Hardarson SH, Stefansson E. Regulation of retinal blood flow in health and disease. *Prog Retin Eye Res*. 2008;27(3):284–330.
- Nguyen TT, Wong TY. Retinal vascular manifestations of metabolic disorders. *Trends Endocrinol Metab*. 2006;17(7):262–8.
- Garcia Garcia LC, Zamorano Martin F, Rocha de Lossada C, et al. Retinitis pigmentosa as a clinical presentation of LCHAD deficiency: a clinical case and review of the literature. *Arch Soc Esp Oftalmol (Engl Ed)*. 2021;96(9):496–499.
- Schmitz-Valckenberg S, Holz FG, Bird AC, Spaide RF. Fundus autofluorescence imaging: review and perspectives. *Retina*. 2008;28(3):385–409.
- Boese EA, Jain N, Jia Y, et al. Characterization of chorioretinopathy associated with mitochondrial trifunctional protein disorders: long-term follow-up of 21 cases. *Ophthalmology*. 2016;123(10):2183–2195.
- Huang D, Lumbroso B, Jia Y, Waheed N. *Optical Coherence Tomography Angiography of the Eye: OCTAngiography*. Boca Raton, FL: CRC Press; 2024.
- Lange N, Bodetko AM, Mozrzymas R, Kowal-Lange A. Ophthalmic symptoms of long-chain 3-hydroxyacyl-CoA dehydrogenase deficiency: a report of three cases. *Case Rep Ophthalmol*. 2024;15(1):310–319.
- Sacconi R, Bandello F, Querques G. Choroidal neovascularization associated with long-chain 3-hydroxyacyl-CoA dehydrogenase deficiency. *Retinal Cases Brief Rep*. 2022;16(1):99–101.
- Tyni T, Kivela T, Lappi M, Summanen P, Nikoskelainen E, Pihko H. Ophthalmologic findings in long-chain 3-hydroxyacyl-CoA dehydrogenase deficiency caused by the G1528C mutation: a new type of hereditary metabolic chorioretinopathy. *Ophthalmology*. 1998;105(5):810–824.
- Jia Y, Tan O, Tokayer J, et al. Split-spectrum amplitude-decorrelation angiography with optical coherence tomography. *Optics Express*. 2012;20(4):4710–4725.
- Spaide RF, Fujimoto JG, Waheed NK, Sadda SR, Staurenghi G. Optical coherence tomography angiography. *Prog Retin Eye Res*. 2018;64:1–55.
- Jia Y, Bailey ST, Hwang TS, et al. Quantitative optical coherence tomography angiography of vascular abnormalities in the living human eye. *Proc Natl Acad Sci USA*. 2015;112(18):E2395–E2402.
- Hwang TS, Zhang M, Bhavsar K, et al. Visualization of 3 distinct retinal plexuses by projection-resolved optical coherence tomography angiography in diabetic retinopathy. *JAMA Ophthalmol*. 2016;134(12):1411–1419.
- Jia Y, Bailey ST, Wilson DJ, et al. Quantitative optical coherence tomography angiography of choroidal neovascularization in age-related macular degeneration. *Ophthalmology*. 2014;121(7):1435–1444.
- Wongchaisuwat N, Wang J, Yang P, et al. Optical coherence tomography angiography of choroidal neovascularization in long-chain 3-hydroxyacyl-CoA dehydrogenase deficiency (LCHADD). *Am J Ophthalmol Case Rep*. 2023;32:101958.
- World Medical A. World Medical Association Declaration of Helsinki: ethical principles for medical research involving human subjects. *JAMA*. 2013;310(20):2191–2194.
- Wongchaisuwat N, Gillingham MB, Yang P, et al. A proposal for an updated staging system for LCHADD retinopathy. *Ophthalmic Genet*. 2024;45(2):140–146.
- Wang J, Hormel TT, Bailey ST, Hwang TS, Huang D, Jia Y. Signal attenuation-compensated projection-resolved OCT angiography. *Biomed Opt Express*. 2023;14(5):2040–2054.
- Zhang M, Wang J, Pechauer AD, et al. Advanced image processing for optical coherence tomographic angiography of macular diseases. *Biomed Opt Express*. 2015;6(12):4661–75.
- Lujan BJ, Roorda A, Croskrey JA, et al. Directional optical coherence tomography provides accurate outer nuclear layer and henle fiber layer measurements. *Retina*. 2015;35(8):1511–1520.
- Hormel TT, Wang J, Bailey ST, Hwang TS, Huang D, Jia Y. Maximum value projection produces better en face OCT angiograms than mean value projection. *Biomed Opt Express*. 2018;9(12):6412–6424.
- Otsu N. A threshold selection method from gray-level histograms. *Automatica*. 1975;11(285–296):23–27.
- Wang J, Hormel TT, Bailey S, Hwang T, Huang D, Jia Y. Quantifying choriocapillaris flow deficits in diabetic retinopathy using projection-resolved optical coherence tomographic angiography. *Invest Ophthalmol Vis Sci*. 2023;64(9):PP0020.
- Wang J, Hormel TT, You Q, et al. Robust non-perfusion area detection in three retinal plexuses using convolutional neural network in OCT angiography. *Biomed Opt Express*. 2020;11(1):330–345.
- Huang D, Chopra V, Lu AT-H, Tan O, Francis B, Varma R. Does optic nerve head size variation affect circum papillary retinal nerve fiber layer thickness measurement by optical coherence tomography? *Invest Ophthalmol Vis Sci*. 2012;53(8):4990–4997.
- Gillingham MB, Weleber RG, Neuringer M, et al. Effect of optimal dietary therapy upon visual function in children with long-chain 3-hydroxyacyl CoA dehydrogenase and trifunctional protein deficiency. *Mol Genet Metab*. 2005;86(1–2):124–133.

29. Elizondo G, Matern D, Vockley J, Harding CO, Gillingham MB. Effects of fasting, feeding and exercise on plasma acylcarnitines among subjects with CPT2D, VLCADD and LCHADD/TFPD. *Mol Genet Metab.* 2020;131(1–2):90–97.
30. Smith EH, Matern D. Acylcarnitine analysis by tandem mass spectrometry. *Curr Protoc Hum Genet.* 2010;64(1):17.8.1–17.8.20.
31. Abdi H, Williams LJ. Principal component analysis. *WIREs Comp Stat.* 2010;2(4):433–459.
32. Tyni T, Paetau A, Strauss AW, Middleton B, Kivela T. Mitochondrial fatty acid beta-oxidation in the human eye and brain: implications for the retinopathy of long-chain 3-hydroxyacyl-CoA dehydrogenase deficiency. *Pediatr Res.* 2004;56(5):744–750.
33. Dulz S, Atiskova Y, Engel P, Wildner J, Tsiakas K, Santer R. Retained visual function in a subset of patients with long-chain 3-hydroxyacyl-CoA dehydrogenase deficiency (LCHADD). *Ophthalmic Genet.* 2021;42(1):23–27.
34. Lejoyeux R, Benillouche J, Ong J, et al. Choriocapillaris: Fundamentals and advancements. *Prog Retin Eye Res.* 2022;87:100997.
35. Babcock SJ, Curtis AG, Gaston G, Elizondo G, Gillingham MB, Ryals RC. The LCHADD mouse model recapitulates early-stage chorioretinopathy in LCHADD patients. *Invest Ophtalmol Vis Sci.* 2024;65(6):33.
36. Gillingham MB, Choi D, Gregor A, et al. Early diagnosis and treatment by newborn screening (NBS) or family history is associated with improved visual outcomes for long-chain 3-hydroxyacylCoA dehydrogenase deficiency (LCHADD) chorioretinopathy. *J Inherit Metab Dis.* 2024;47(4):746–756.
37. Chung H, Choi D, Gregor A, et al. Plasma metabolomics, lipidomics, and acylcarnitines are associated with vision and genotype but not with dietary intake in long-chain 3-hydroxyacyl-CoA dehydrogenase deficiency (LCHADD). *J Inherit Metab Dis.* 2025;48(4):e70060.
38. Schoors S, Bruning U, Missiaen R, et al. Fatty acid carbon is essential for dNTP synthesis in endothelial cells. *Nature.* 2015;520(7546):192–197.